Supplementary Information

Electrolyte-free dye sensitized solar cell with high open circuit voltage using a bi-functional ferrocene based cyanovinyl molecule as dye and redox couple.

A. Ghosh,[a] S. Mishra, S. Giri,[b] S. M. Mobin,[c] A. Bera,*[d] S. Chatterjee *[a]

[a]Department of Chemistry, National Institute of Technology Rourkela, Orissa 769008, India.
[b]Theoretical Chemistry Laboratory, Department of Chemistry, National Institute of Technology Rourkela, Orissa-769008, India.
[c]Discipline of Chemistry, Indian Institute of Technology Indore, Simrol, Madhya Pradesh 452017, India.
[d]Department of Physics, Indian Institute of Technology Jammu, Jammu, Jammu & Kashmir 181121, India.

*Corresponding author. Tel.: +91 661 2462656; Fax : +91 661 2472926
E-mail address: saurav@nitrkl.ac.in, ashok.bera@iitjammu.ac.in

Contents:

Figure S1: ^{1}H NMR of Compound 1

Figure S2: ^{1}H NMR of Compound 2

Figure S3: ^{1}H NMR of Compound 3

Figure S4: ^{1}H NMR of Compound 4

Figure S5: ^{1}H NMR of Compound 5

Figure S6: Molecular Structure of 2

Figure S7: Cyclic voltammograms (—) and differential pulse voltammograms (…)

Figure S8: DFT optimized structure of 1 and 2.

Table S1: Gross electron population on the neutral and oxidised species of compounds 1 and 2.

Figure S9: Correlation of UV-Visible absorption spectra of compounds 1 and 2 using TD-DFT

Table S2 : Calculation of Orbital contribution (%)

Table S3: Excitation energies and oscillator strengths of 1

Table S4: Excitation energies and oscillator strengths of 2

Figure S10: Diode like characteristics of TiO_2/[1],[2]/Pt in Dark condition

Figure S11: FE SEM Images of FTO/TIO_2 layer deposited with compound (a) 1 and (b) 2

Figure S12: Band Gap calculation of (a) 1 and (b) 2 using Tauc's Plot.

Figure S13: UV –Visible Spectra of compounds 1 and 2 in Dichloromethane solution

Figure S14: Thin film absorption spectra of 1, 2 and ferrocene (Fc).

Figure S15: Schematic of the TiO_2/[1],[2]/Pt meso-heterojunction solar cells.

Figure S16: Proposed electron transfer processes.

Table S5 : Frontier Molecular orbitals of 1, 1^+, 2 and 2^+.

Table S6: Geometry optimized coordinates for compound 1

Table S7: Geometry optimized coordinates for compound 2

Text S1: Experimental Sections

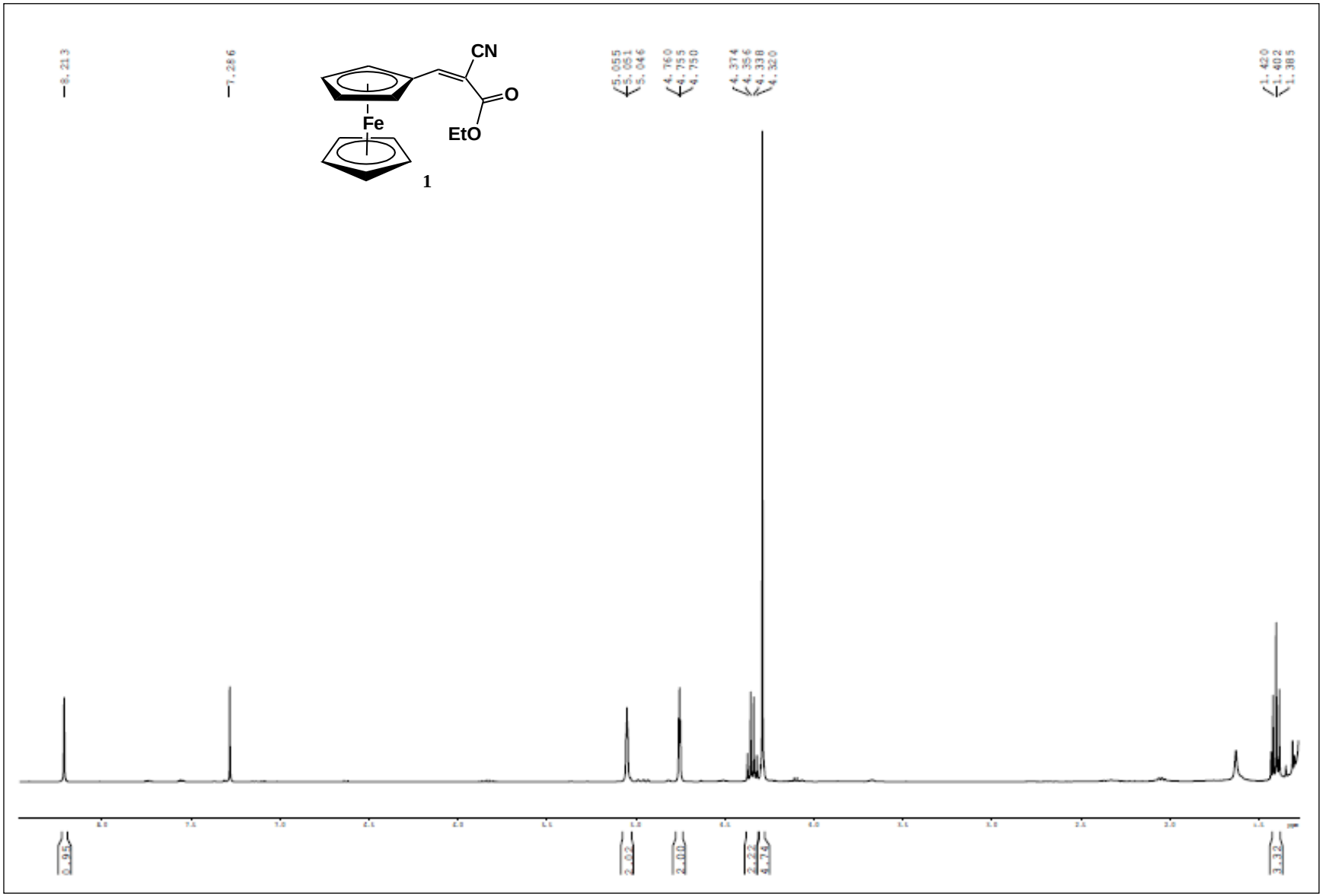

Figure S1: ^{1}H NMR ($CDCl_3$, 400 MHz) of Compound 1

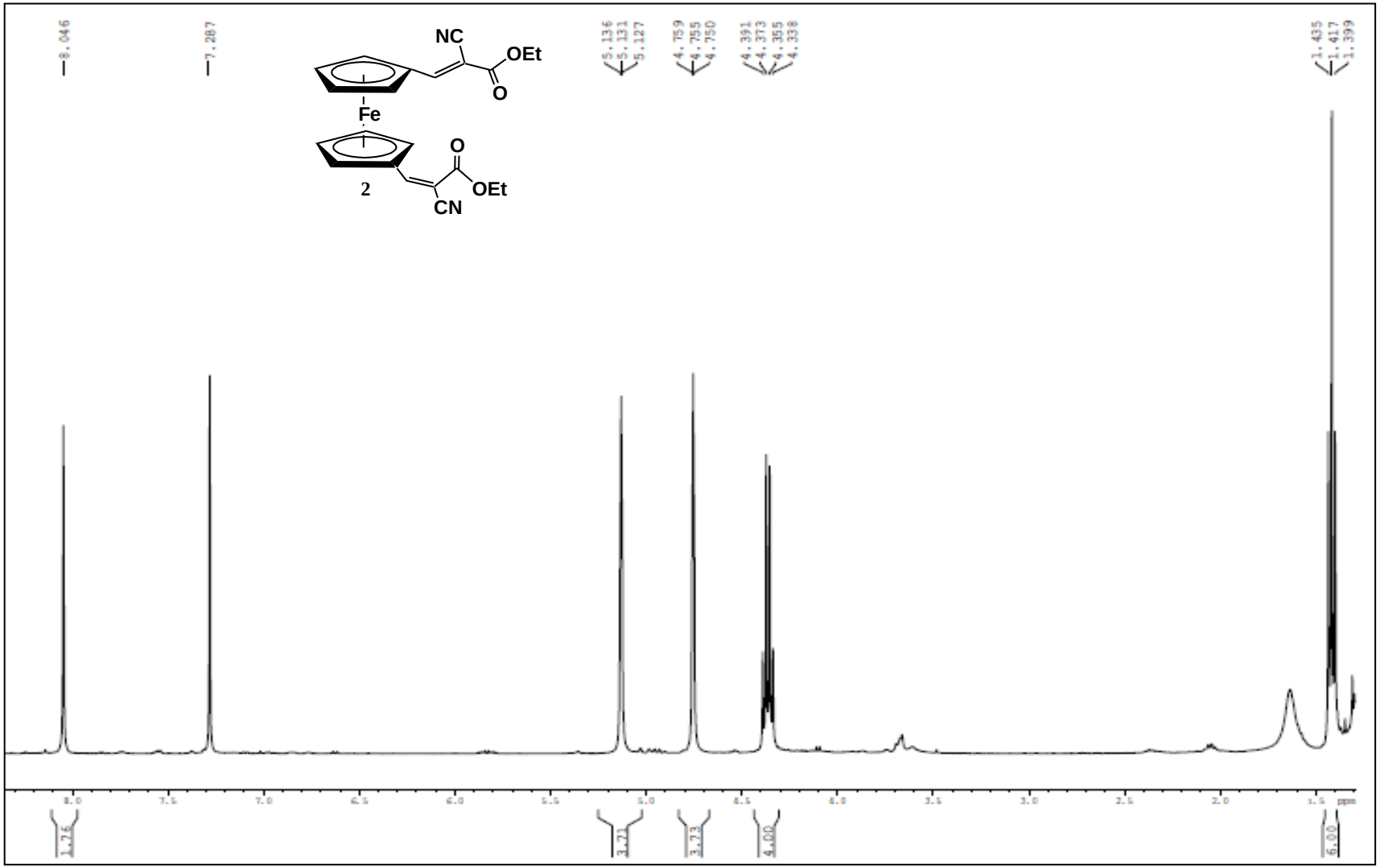

Figure S2: ^{1}H NMR ($CDCl_3$, 400 MHz) of Compound 2

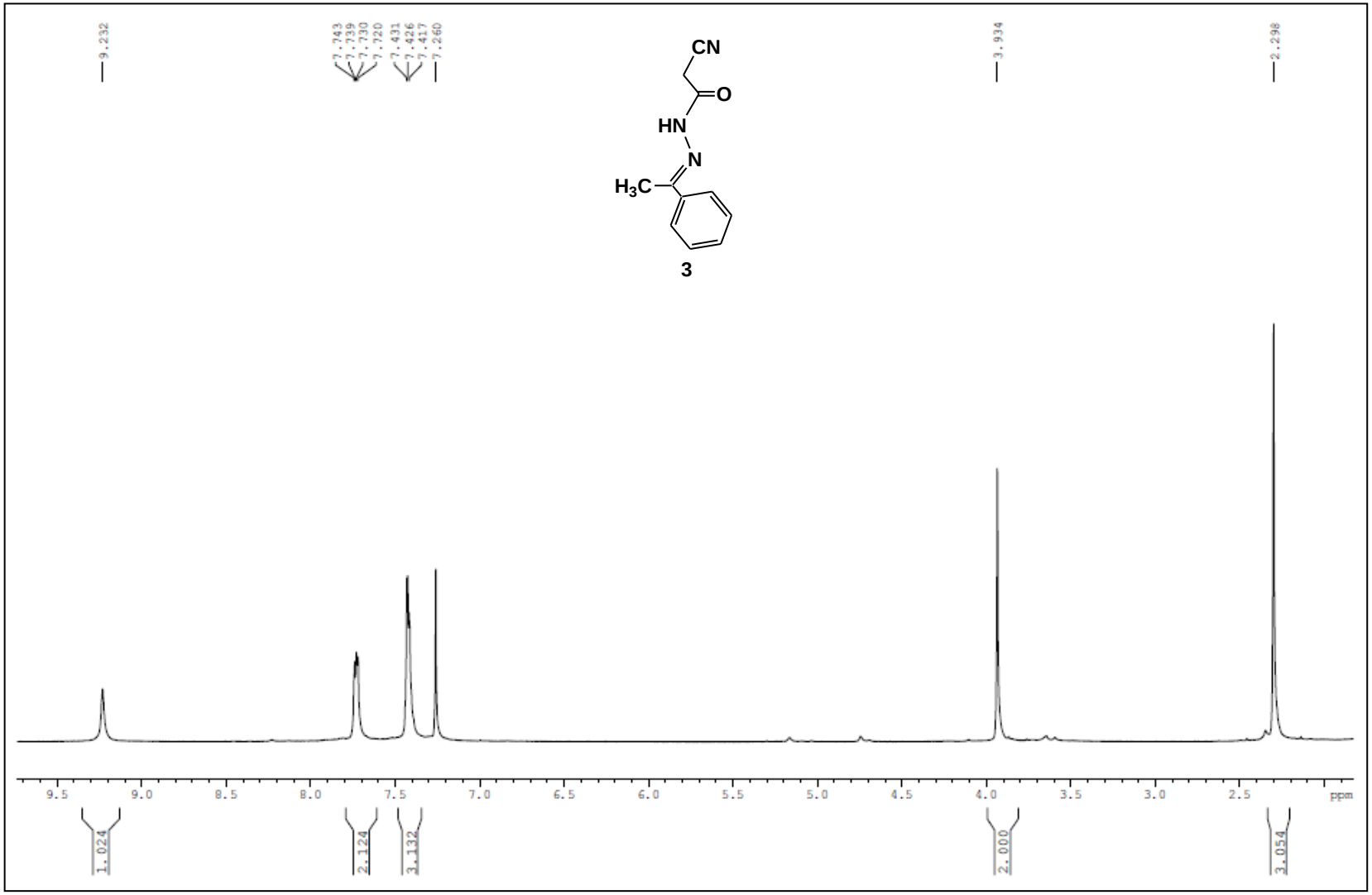

Figure S3: ^{1}H NMR ($CDCl_3$, 400 MHz) of Compound 3

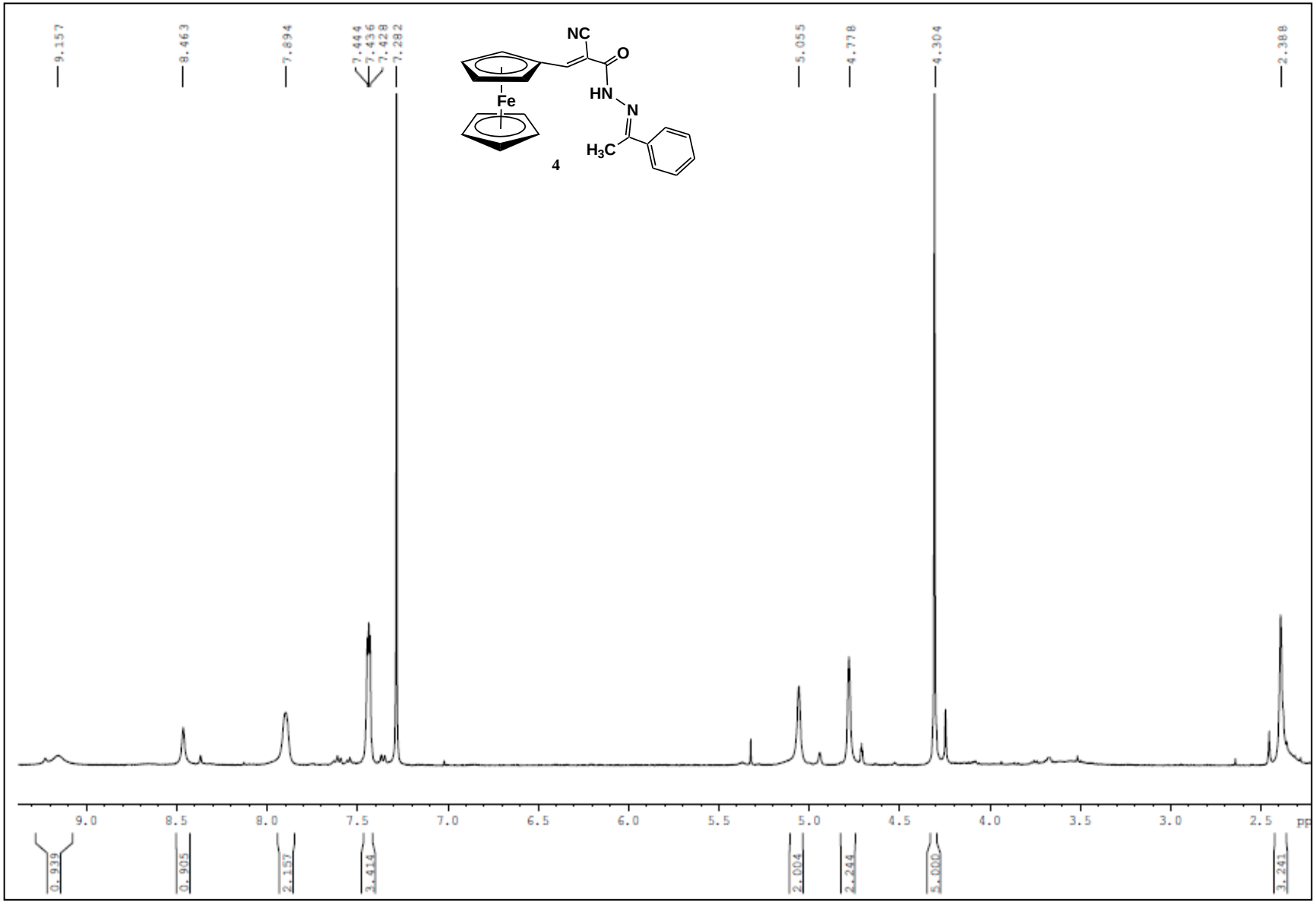

Figure S4: ^{1}H NMR ($CDCl_3$, 400 MHz) of Compound 4

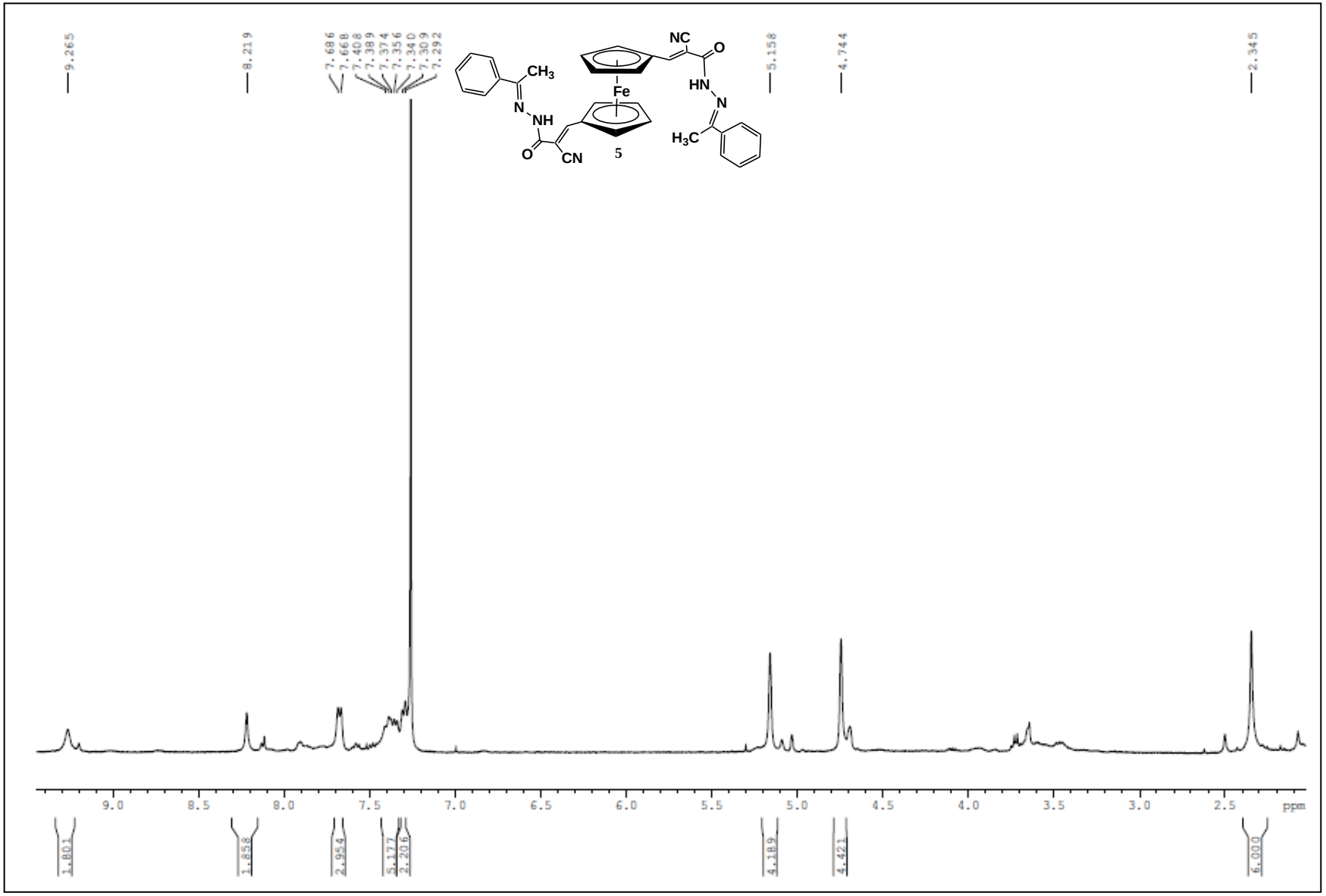

Figure S5: ^{1}H NMR ($CDCl_3$, 400 MHz) of Compound 5

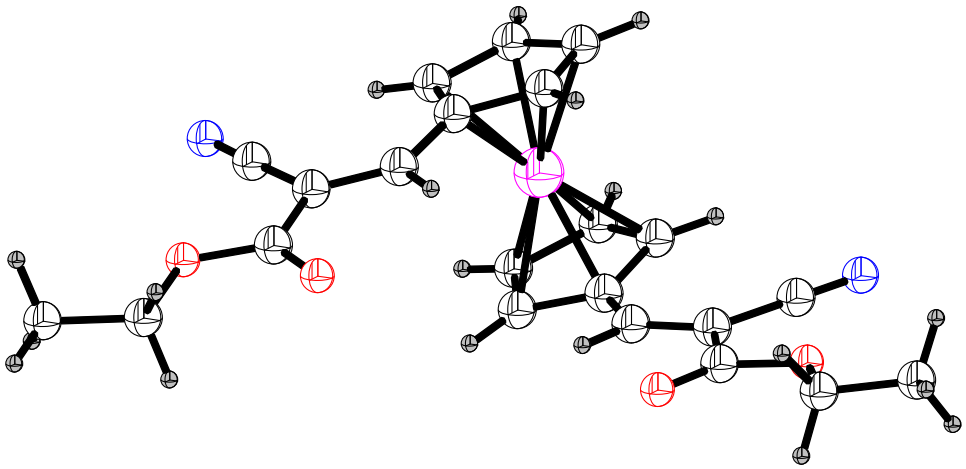

Figure S6: Molecular Structure of 2

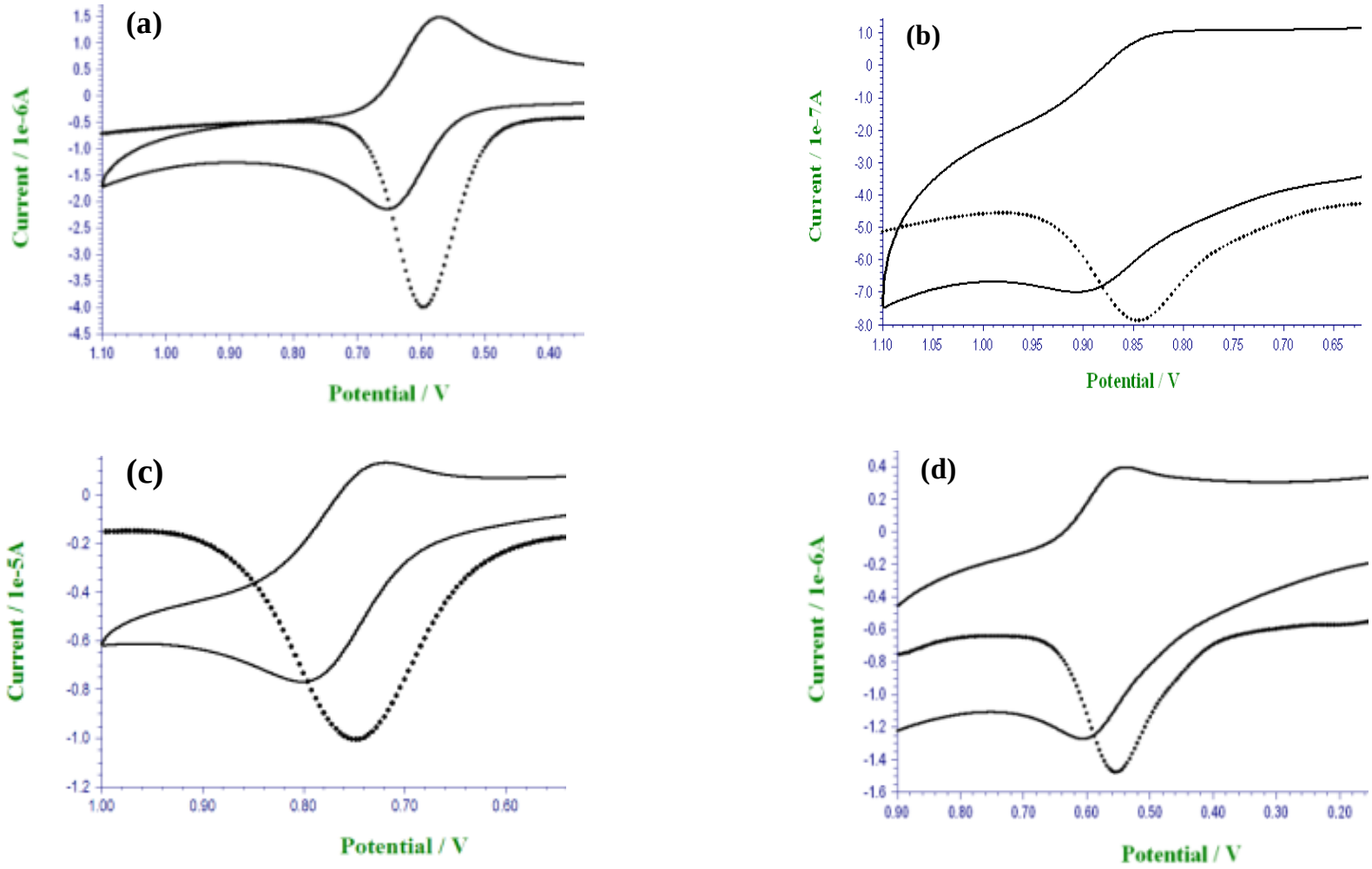

Figure S7: Cyclic voltammograms (—) and differential pulse voltammograms (…) of compounds (a)1, (b)2, (c)4, (d)5 in Acetonitrile / 0.1 M TBAP at 298 K vs SCE. Under the same conditions, the potential of the Ferrocenium/Ferrocene couple was 0.37 V versus SCE.

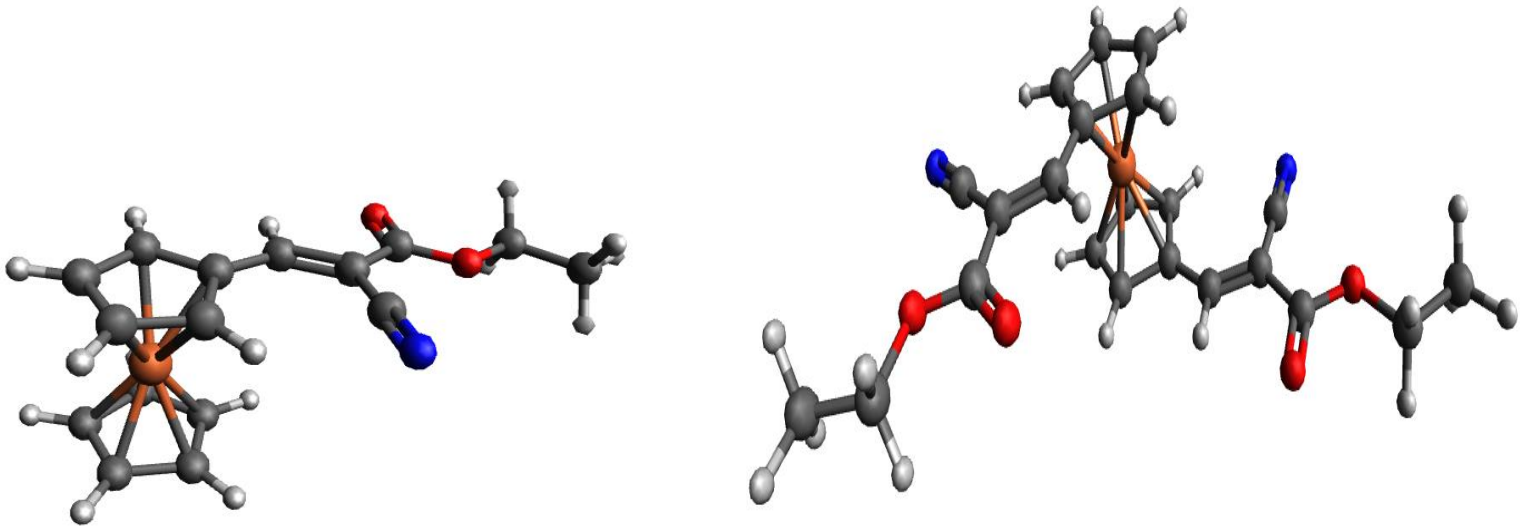

Figure S8: DFT optimized structure of 1 and 2.

Table S1: Gross electron population on the neutral and oxidised species of compounds 1 and 2.

Neutral (**1**)		Oxidised (**1**$^+$)		
Fe	$CHC(CN)CO_2Et$	Spin	Fe	$CHC(CN)CO_2Et$
26.17438	64.32577	α	13.61445	32.46797
		β	12.35951	32.48862
		α–β	1.25494	-0.02065
Neutral (**2**)		Oxidised (**2**$^+$)		
Fe	{$CHC(CN)CO_2Et$}/ {$CHC(CN)CO_2Et$}	Spin	Fe	{$CHC(CN)CO_2Et$}/ {$CHC(CN)CO_2Et$}
26.13880	65.094/ 64.32209	α	13.618	33.1206/ 32.4623
		β	12.3221	32.48775/ 32.48774
		α–β	1.29594	0.63285/ -0.02546

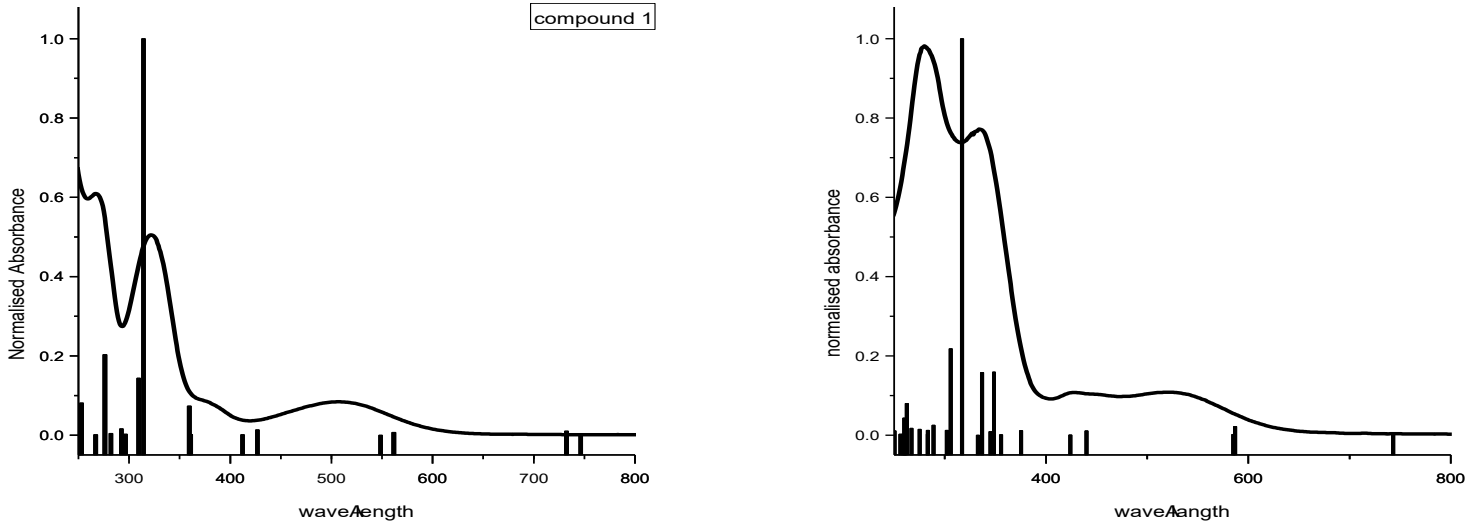

Figure S9: Correlation of UV-Visible absorption spectra of compounds 1 and 2 using TD-DFT

Table S2 : Calculation of Orbital contribution (%)

MO's	CH	Ferocene	CHCN	Ester
HOMO (**1**)	0	93	1	3
LUMO (**1**)	34	28	21	17
HOMO (**2**)	0	87	11	2
LUMO (**2**)	32	31	22	15

Table S3: Excitation energies and oscillator strengths of 1

```
(75= HOMO: 76 = LUMO)
 Excited State   1:      Singlet-A      1.6610 eV  746.42 nm  f=0.0001  <S**2>=0.000
      74 -> 76         0.43641
      75 -> 77         0.35912

 Excited State   2:      Singlet-A      1.6932 eV  732.26 nm  f=0.0046  <S**2>=0.000
      74 -> 77         0.38435
      75 -> 78         0.42484

 Excited State   3:      Singlet-A      2.2074 eV  561.67 nm  f=0.0030  <S**2>=0.000
      71 -> 78         0.33564
      74 -> 77         0.45881
      75 -> 76         0.21723

 Excited State   4:      Singlet-A      2.2603 eV  548.52 nm  f=0.0001  <S**2>=0.000
      71 -> 77         0.33804
      74 -> 78         0.14183
      75 -> 77         0.51133

 Excited State   5:      Singlet-A      2.9045 eV  426.87 nm  f=0.0059  <S**2>=0.000
      71 -> 76         0.33174
      74 -> 77         0.31816
      75 -> 76         0.37716

 Excited State   6:      Singlet-A      3.0084 eV  412.12 nm  f=0.0004  <S**2>=0.000
      71 -> 77         0.39742
      72 -> 77         0.11534
      74 -> 76         0.45283
      74 -> 78         0.29314

 Excited State   7:      Singlet-A      3.4351 eV  360.94 nm  f=0.0009  <S**2>=0.000
```

```
     74 -> 76         0.17161
     74 -> 78         0.46383
     75 -> 77         0.27100

 Excited State   8:      Singlet-A      3.4485 eV  359.53 nm  f=0.0327  <S**2>=0.000
     71 -> 78         0.11095
     75 -> 76         0.32943
     75 -> 78         0.52350

 Excited State   9:      Singlet-A      3.9449 eV  314.29 nm  f=0.4451  <S**2>=0.000
     70 -> 76         0.11371
     72 -> 76         0.24820
     73 -> 76         0.62373
     75 -> 76         0.14891

 Excited State  10:      Singlet-A      4.0073 eV  309.40 nm  f=0.0641  <S**2>=0.000
     72 -> 76         0.61893

 Excited State  11:      Singlet-A      4.1819 eV  296.48 nm  f=0.0012  <S**2>=0.000
     69 -> 76         0.68847
Excited State  12:      Singlet-A      4.2399 eV  292.42 nm  f=0.0071  <S**2>=0.000
     71 -> 76         0.41323
     71 -> 78         0.40676
     72 -> 78         0.12816

 Excited State  13:      Singlet-A      4.3949 eV  282.11 nm  f=0.0020  <S**2>=0.000
     68 -> 76         0.65149

 Excited State  14:      Singlet-A      4.4902 eV  276.12 nm  f=0.0905  <S**2>=0.000
     68 -> 77         0.10564
     70 -> 76         0.58187
     71 -> 76         0.21818
     71 -> 78         0.19291

 Excited State  15:      Singlet-A      4.6427 eV  267.05 nm  f=0.0005  <S**2>=0.000
     71 -> 77         0.15013
     73 -> 77         0.66916
```

Table S4: Excitation energies and oscillator strengths of compound 2

(107 = HOMO; 108= LUMO)

```
 Excited State   1:      Singlet-A      1.6109 eV  769.68 nm  f=0.0004  <S**2>=0.000
     106 ->108         0.42113
     106 ->111         0.35255
     107 ->110         0.32160

 Excited State   2:      Singlet-A      1.6686 eV  743.03 nm  f=0.0014  <S**2>=0.000
     106 ->109         0.27193
     107 ->108         0.36627
     107 ->111         0.36171

 Excited State   3:      Singlet-A      2.1125 eV  586.90 nm  f=0.0160  <S**2>=0.000
     103 ->108         0.27340
     103 ->111         0.28682
     106 ->108         0.29666
     106 ->111         0.18587
     107 ->109         0.31882

 Excited State   4:      Singlet-A      2.1190 eV  585.11 nm  f=0.0010  <S**2>=0.000
     103 ->110         0.28638
     105 ->110         0.12064
     106 ->109         0.33333

 Excited State   5:      Singlet-A      2.8170 eV  440.13 nm  f=0.0078  <S**2>=0.000
     103 ->108         0.38780
     103 ->111         0.32735
     105 ->108         0.21430

 Excited State   6:      Singlet-A      2.9243 eV  423.98 nm  f=0.0003  <S**2>=0.000
     103 ->110         0.39252
     105 ->110         0.11398
     107 ->108         0.29701

 Excited State   7:      Singlet-A      3.3036 eV  375.30 nm  f=0.0083  <S**2>=0.000
     106 ->111         0.38047
```

```
    107 ->109         0.37902
    107 ->110         0.29627

Excited State   8:      Singlet-A      3.4860 eV  355.66 nm  f=0.0005  <S**2>=0.000
    106 ->109         0.43911
    106 ->110         0.47214
    107 ->108         0.15916

Excited State   9:      Singlet-A      3.5562 eV  348.64 nm  f=0.1178  <S**2>=0.000
    103 ->108         0.17097
    106 ->108         0.18193
    107 ->109         0.25436
    107 ->110         0.42274

Excited State  10:      Singlet-A      3.5929 eV  345.08 nm  f=0.0064  <S**2>=0.000
    103 ->110         0.15668
    105 ->109         0.17182
    106 ->110         0.18048
    107 ->111         0.50344

Excited State  11:      Singlet-A      3.6808 eV  336.84 nm  f=0.1171  <S**2>=0.000
    105 ->108         0.56309

Excited State  12:      Singlet-A      3.7261 eV  332.75 nm  f=0.0000  <S**2>=0.000
    104 ->108         0.53470
    106 ->110         0.10329
    107 ->111         0.19233

Excited State  13:      Singlet-A      3.9112 eV  317.00 nm  f=0.7413  <S**2>=0.000
    104 ->109         0.58469
    105 ->108         0.33096
    107 ->109         0.13900

Excited State  14:      Singlet-A      4.0544 eV  305.80 nm  f=0.1616  <S**2>=0.000
    104 ->108         0.36094
    105 ->109         0.47052
    107 ->108         0.15346
```

```
Excited State  15:      Singlet-A      4.1010 eV  302.33 nm  f=0.0035  <S**2>=0.000
    101 ->108         0.50551

Excited State  16:      Singlet-A      4.1035 eV  302.14 nm  f=0.0088  <S**2>=0.000
    102 ->108         0.48261
    105 ->109         0.10845

Excited State  17:      Singlet-A      4.2913 eV  288.92 nm  f=0.0183  <S**2>=0.000
     99 ->108         0.53808
     99 ->111         0.17918
    103 ->108         0.20847
```

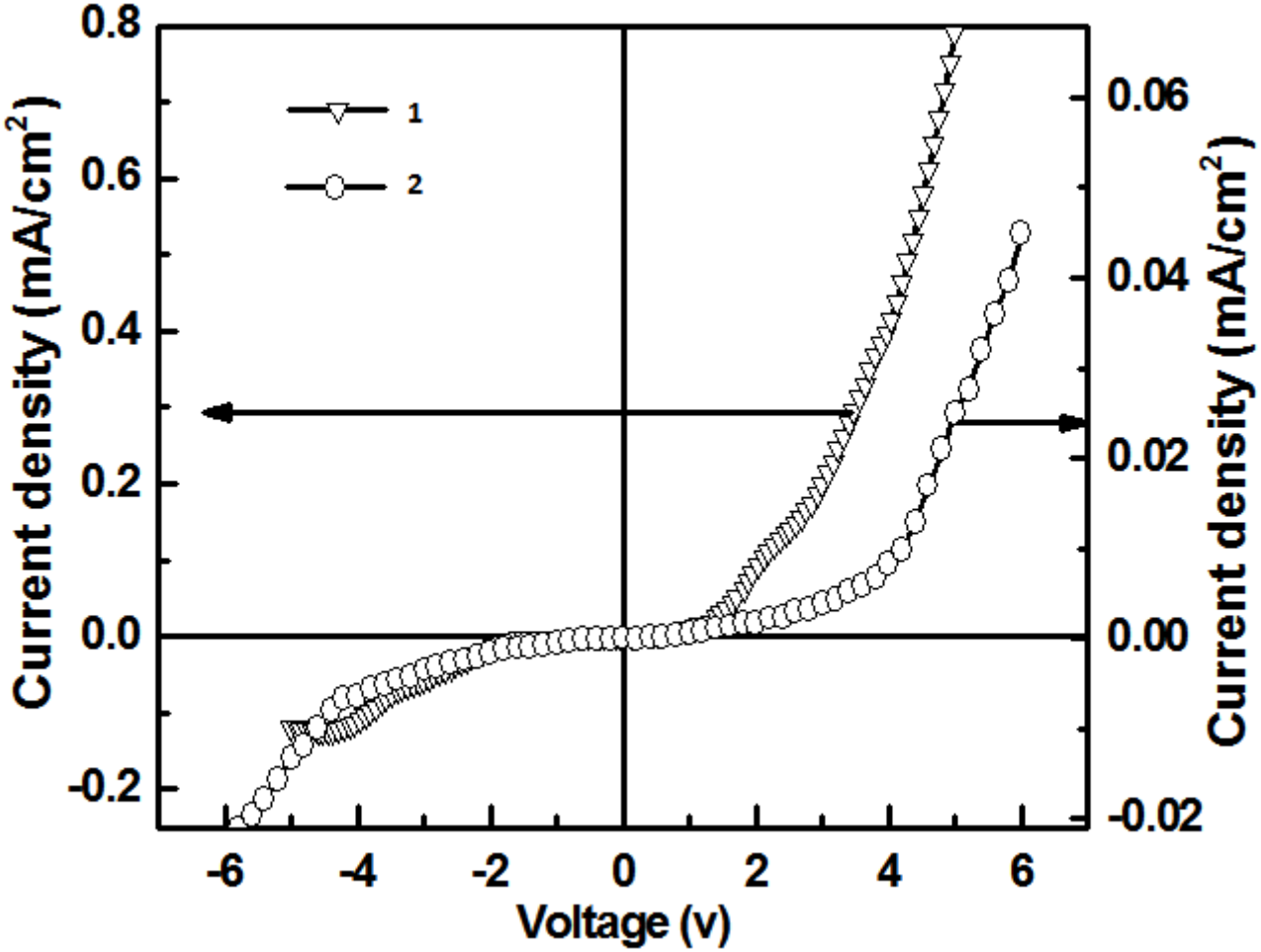

Figure S10: Diode like characteristics of TiO_2/[1],[2]/Pt in Dark condition

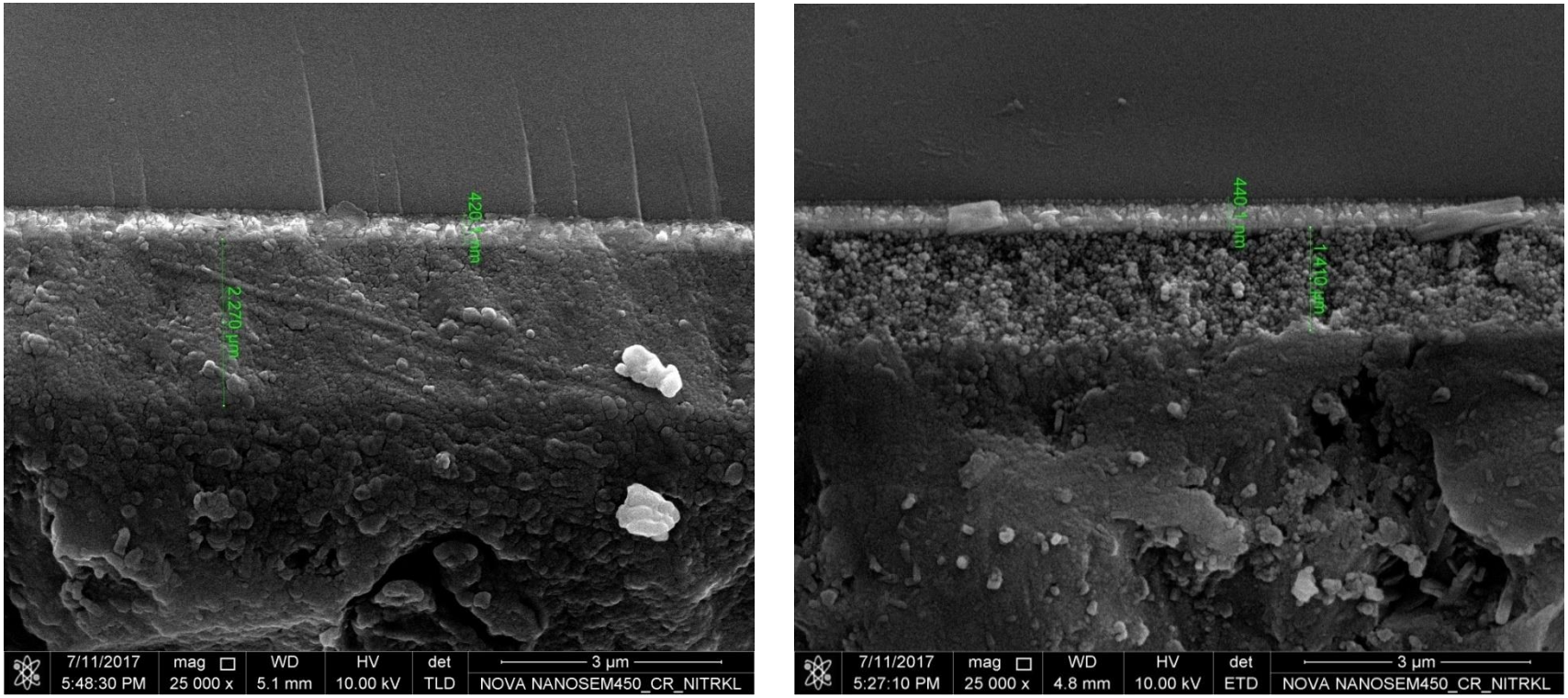

Figure S11: FE SEM Images of FTO/TIO_2 layer deposited with compound (a) 1 and (b) 2

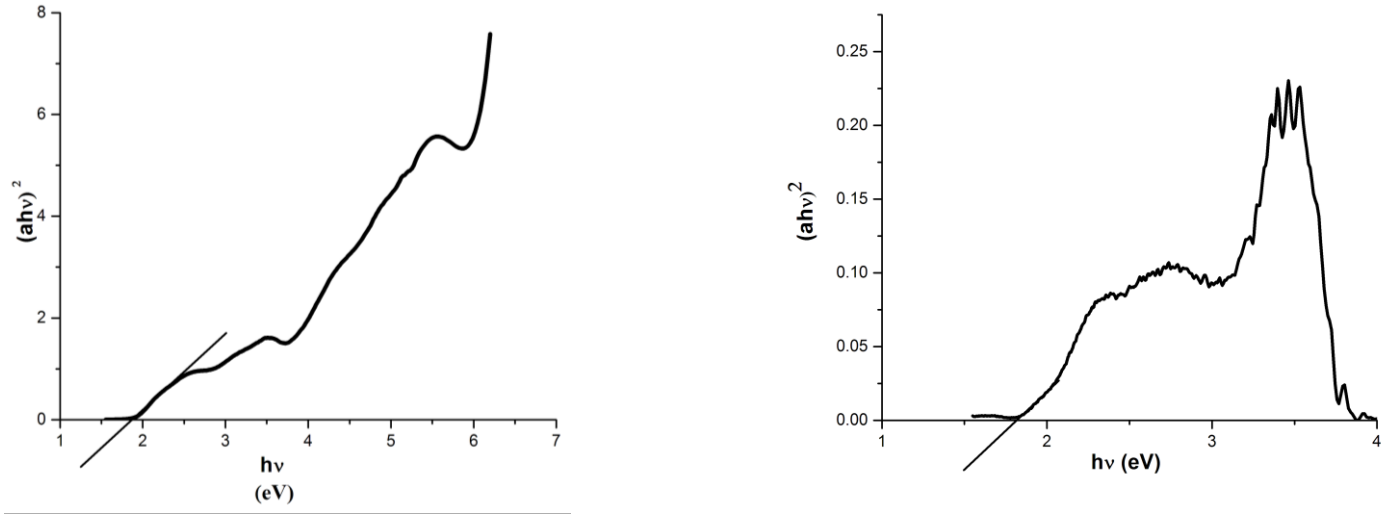

(a) **(b)**

Figure S12: Band Gap calculation of (a) 1 and (b) 2 using Tauc's Plot as per reference [1, 2]

1. Dongol, M.; El-Nahass, M. M; El-Denglawey, A; Elhady, A. F; Abuelwafa, A. A. Optical Properties of Nano 5,10,15,20-Tetraphenyl-21H,23H-Prophyrin Nickel (II) Thin Films, Curr. Appl. Phys. **2012**, *12*, 1178 and the references therein.

2. Kim, H-S; Lee, C-R; Im, J-H; Lee, K-B; Moehl, T; Marchioro, A; Moon, S-J; Humphry-Baker, R.; Yum, J-H; Moser, J. E; Gratzel, M; Park, N-G. Lead Iodide Perovskite Sensitized All-Solid-State Submicron Thin Film Mesoscopic Solar Cell with Efficiency Exceeding 9%, Sci Rep.**2012**, *2*, 2-7.

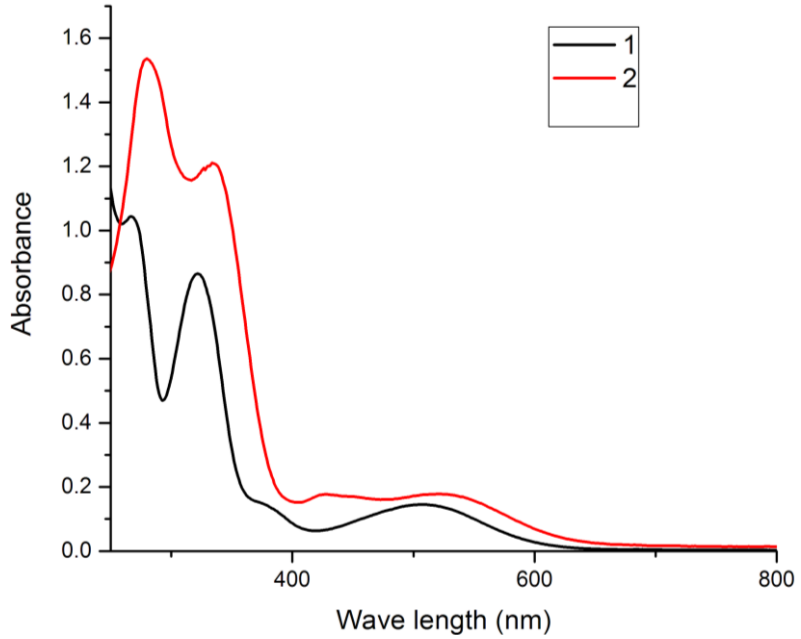

Figure S13: UV –Visible Spectra of compounds 1 and 2 in 2x10^{-5} [M] dichloromethane solution

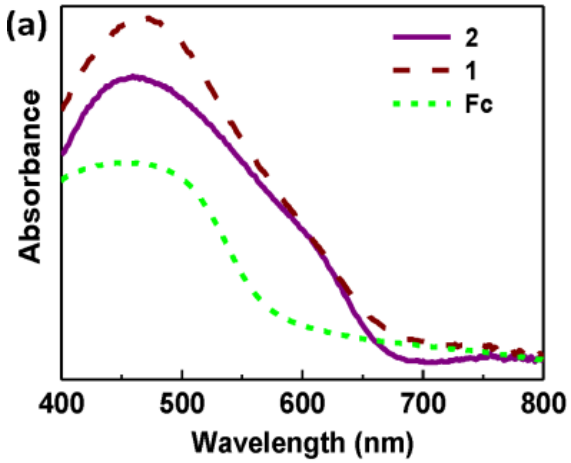

Figure S14: Thin film absorption spectra of 1, 2 and ferrocene (Fc).

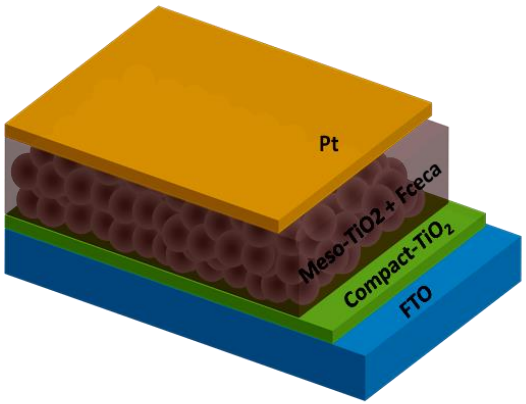

Figure S15: Schematic of the TiO_2/[1],[2]/Pt meso-heterojunction solar cells.

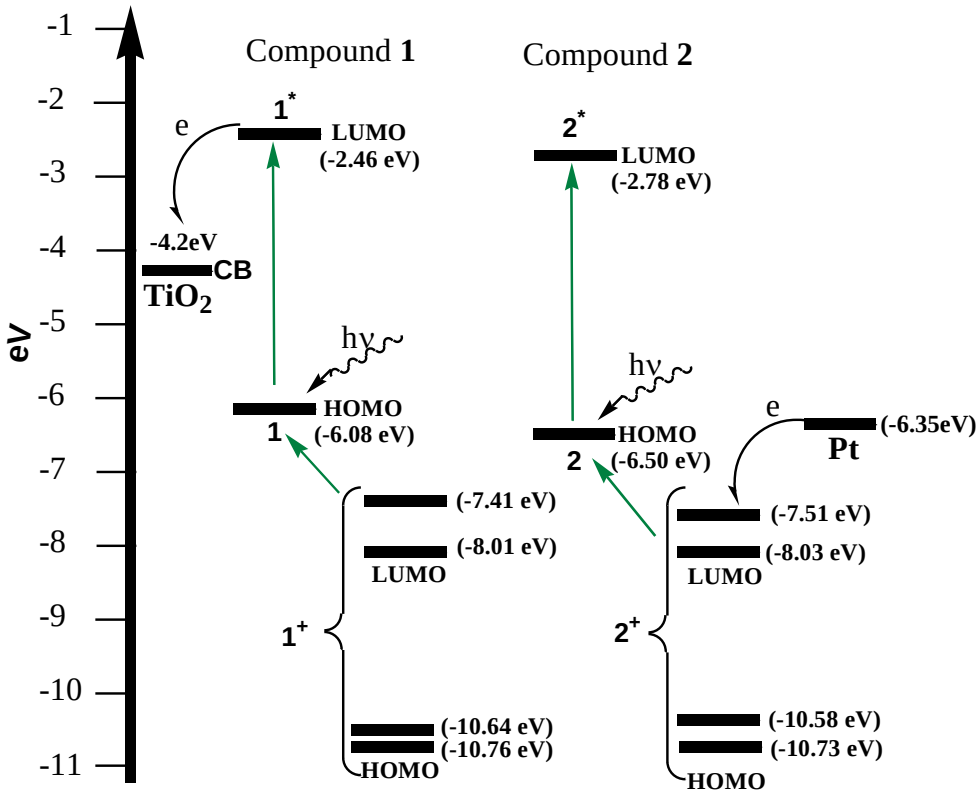

Figure S16: Proposed electron transfer processes

Table S5 : Frontier Molecular orbitals of 1, 1^+, 2 and 2^+.

	[1]	[1^+]	
		α	β
LUMO	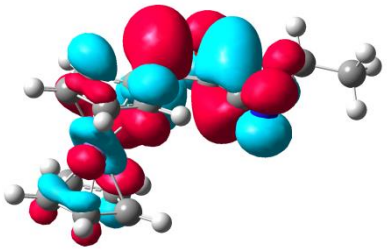 -2.46 eV	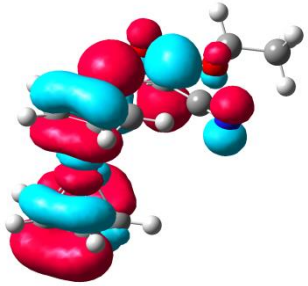 -7.41 eV	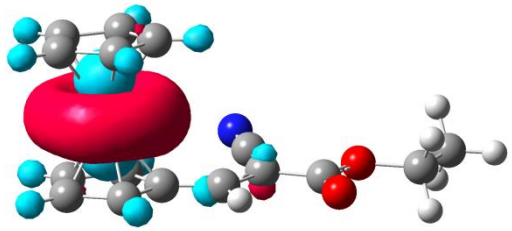 -8.01 eV
HOMO	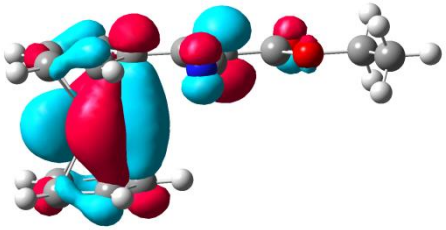 -6.08 eV	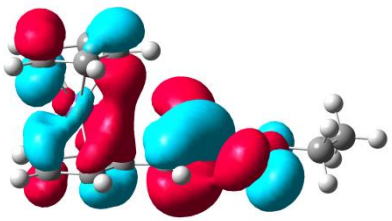 -10.64 eV	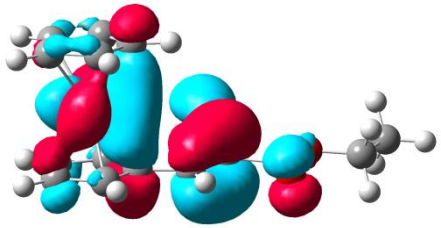 -10.76 eV
	[2]	[2^+]	
		α	β
LUMO	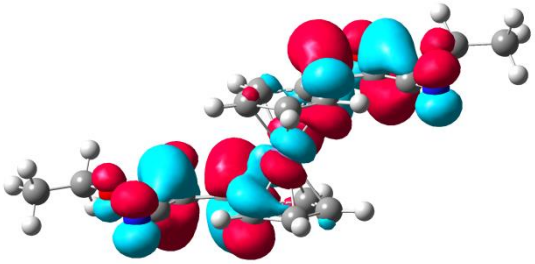	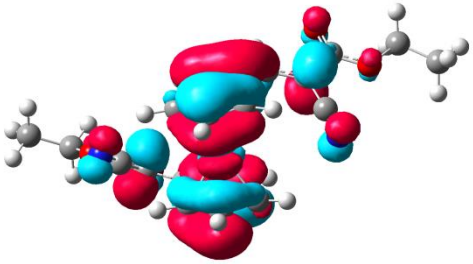	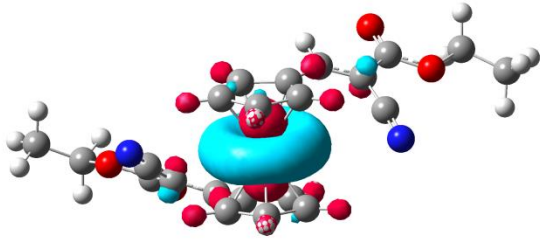

	-2.78 eV	-7.51 eV	-8.03 eV
HOMO	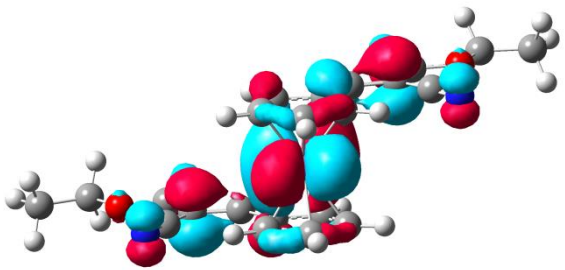 **-6.50 eV**	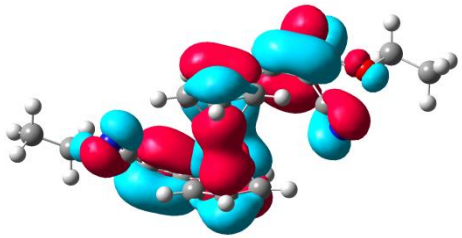 **-10.58 eV**	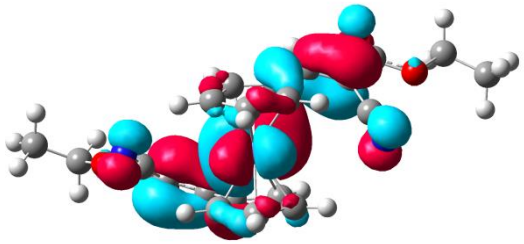 **-10.73 eV**

<u>Table S6: Geometry optimized coordinates for compound 1</u>

```
Standard orientation:
 ---------------------------------------------------------------------
 Center     Atomic      Atomic              Coordinates (Angstroms)
 Number     Number       Type              X           Y           Z
 ---------------------------------------------------------------------
```

1	26	0	-2.240218	-0.060647	-0.014777
2	8	0	4.080541	-0.097981	0.111402
3	8	0	3.094794	-0.472998	-1.943970
4	6	0	-0.625541	1.170077	-0.610051
5	6	0	-3.500774	-1.208861	1.240579
6	1	0	-4.178692	-0.800030	1.976806
7	6	0	-2.625366	-2.003863	-0.773143
8	6	0	-2.540898	2.002142	0.442593
9	1	0	-3.213610	2.389869	1.194413
10	6	0	1.866033	0.960314	1.216990
11	6	0	-3.811907	-1.476298	-0.142670
12	1	0	-4.764027	-1.302131	-0.624248
13	6	0	1.809659	0.542237	-0.152593
14	7	0	1.882542	1.305813	2.348856
15	6	0	-1.170803	1.639615	0.657975
16	1	0	-0.636445	1.715897	1.592054
17	6	0	-1.583785	-2.065687	0.223841
18	1	0	-0.568054	-2.398316	0.060529
19	6	0	0.682070	0.647035	-0.931814
20	1	0	0.806423	0.282561	-1.952643
21	6	0	-1.704549	1.235744	-1.590205
22	1	0	-1.616197	0.958595	-2.631915
23	6	0	5.361198	-0.674619	-0.376692
24	1	0	5.698344	-0.080434	-1.234000
25	1	0	5.166798	-1.697347	-0.720171
26	6	0	6.337973	-0.623903	0.791520
27	1	0	6.491815	0.407965	1.125289
28	1	0	7.306174	-1.039665	0.483494
29	1	0	5.961634	-1.207286	1.638866
30	6	0	-2.871454	1.754864	-0.942478
31	1	0	-3.832056	1.928010	-1.406095
32	6	0	-2.121734	-1.571909	1.467169
33	1	0	-1.585185	-1.484888	2.401418
34	6	0	3.026772	-0.054543	-0.769890
35	1	0	-2.533108	-2.302892	-1.807839

Table S7: Geometry optimized coordinates for compound 2

Standard orientation:

Center Number	Atomic Number	Atomic Type	Coordinates (Angstroms) X	Y	Z
1	26	0	0.000162	-1.787189	-0.000058
2	8	0	5.272119	1.757680	-0.104687
3	8	0	-5.272124	1.757531	0.105171
4	8	0	-3.343116	2.844972	-0.554734
5	8	0	3.342978	2.844910	0.555179
6	6	0	1.368661	-0.873194	1.340170
7	6	0	-0.566940	-3.052881	-1.615674
8	1	0	-0.502581	-4.131728	-1.612926
9	6	0	-1.368538	-0.872961	-1.339977
10	6	0	0.567011	-3.053161	1.615445
11	1	0	0.502683	-4.132010	1.612579
12	6	0	4.256020	-0.708110	0.249462
13	6	0	-1.692091	-2.284108	-1.170664
14	1	0	-2.618005	-2.684477	-0.788341
15	6	0	3.427282	0.419814	0.558614
16	7	0	4.912711	-1.658005	-0.008928
17	6	0	1.692224	-2.284338	1.170695
18	1	0	2.618210	-2.684618	0.788460
19	6	0	-0.014901	-0.808455	-1.875972
20	1	0	0.520053	0.102751	-2.108584
21	6	0	2.142779	0.309404	1.030871
22	1	0	1.644524	1.263308	1.210452
23	6	0	0.014955	-0.808773	1.875996
24	1	0	-0.520062	0.102385	2.108653
25	6	0	5.950550	3.059903	-0.347563
26	1	0	5.941211	3.628203	0.589673
27	1	0	5.368579	3.613187	-1.093736
28	6	0	7.360995	2.737204	-0.824092
29	1	0	7.905814	2.163345	-0.066698
30	1	0	7.908409	3.668956	-1.016817

31	1	0	7.335532	2.150554	-1.748806
32	6	0	-0.470683	-2.144970	2.048437
33	1	0	-1.441345	-2.424646	2.431845
34	6	0	-5.950672	3.059675	0.348095
35	1	0	-5.940184	3.628627	-0.588729
36	1	0	-5.369484	3.612370	1.095324
37	6	0	0.470702	-2.144632	-2.048681
38	1	0	1.441302	-2.424268	-2.432279
39	6	0	-7.361693	2.736848	0.822844
40	1	0	-7.905799	2.163697	0.064402
41	1	0	-7.909144	3.668543	1.015734
42	1	0	-7.337327	2.149447	1.747112
43	6	0	3.976556	1.790884	0.347683
44	6	0	-3.976590	1.790881	-0.347308
45	6	0	-2.142683	0.309582	-1.030545
46	6	0	-3.427239	0.419864	-0.558417
47	6	0	-4.255973	-0.708150	-0.249574
48	7	0	-4.912630	-1.658132	0.008584
49	1	0	-1.644422	1.263535	-1.209894

Text S1: Experimental Sections

1.1. General Procedures

All reactions and manipulations were carried out under an inert atmosphere of dry, pre-purified argon using standard Schlenk line techniques. Solvents were purified, dried and distilled under argon atmosphere prior to use. Infrared spectra were recorded on a Perkin Elmer Spectrum 2 spectrometer as CH_2Cl_2 solution and NMR spectra on a 400 MHz Bruker spectrometer in $CDCl_3$ solvent. Elemental analyses were performed on a Vario El Cube analyser. Mass spectra were obtained on a SQ-300 MS instrument operating in ESI mode. UV-Visible spectroscopy was measured using Shimadzu UV2450. Cyclic voltammetric and differential pulse voltammetric measurements were carried out using a CH Instruments model 600D electrochemistry system. A platinum working electrode, a platinum wire auxiliary electrode and a standard calomel reference electrode were used in a three–electrode configuration. The supporting electrolyte used was 0.1 M $[NBu_4]ClO_4$ and the solute concentration was ~10^{-3} M. The electrochemical experiments were scanned in the positive potential from 0 to +1.2 V and the scan rate used was 50 mV s^{-1}. All the electrochemical experiments were carried out under a nitrogen atmosphere and are uncorrected for junction potentials. The surface morphology of the deposited FTO/TiO_2 thin film was examined using field emission scanning electron microscope (FE-SEM) Nova NanoSEM 450, FEI. $[(\eta^5\text{-}C_5H_5)Fe(\eta^5\text{-}C_5H_4CHO)]$, $[Fe(\eta^5\text{-}C_5H_4)_2(CHO)_2]$ were prepared following reported procedures.[1]

*1.2. Synthesis of 1-[{(η^5-C_5H_5)Fe(η^5-C_5H_4)CH=C(CN)COR}], {R = OEt (**1**), -NHN=C(CH_3)C_6H_5 (**4**)} and 1,1'-[Fe{(η^5-C_5H_4)CH=C(CN)COR}$_2$], {R = OEt (**2**), -NHN=C(CH_3)C_6H_5 (**5**)}*

In a typical reaction procedure, 100 ml round bottomed flask containing 2 gm of Red mud (RM), solution of ferrocenyl carboxyldehyde (0.5 mmol, 107 mg) or 1,1'-ferrocenyl dicarboxyldehyde (0.5 mmol, 121 mg) was added. The mixture was thoroughly mixed using a magnetic stirrer and the solvent was evacuated using vacuum to obtain a solid mixture. Ethylcyanoacetate (0.5 mmol/1 mmol, 57 mg/ 113 mg) or [{$(C_6H_5)C(CH_3)$=NNHC(O)CH_2CN}] (**3**) (0.5 mmol/1 mmol, 101 mg/ 201 mg) was then added to the solid reaction mixture and stirred continuously for one hour at room temperature condition. After the reaction, the solid reaction mixture was extracted in ethyl acetate and the solution was dried in vacuum. The residue was then dissolved in dichloromethane and subjected to short column chromatography to purify the compounds. Elution with 20% ethylacetate : n-hexane solvent mixture afforded the respective violet colored compounds, 1-[{(η^5-C_5H_5)Fe(η^5-C_5H_4)CH=C(CN)COR}], {R = OEt (**1**), -NHN=C(CH_3)C_6H_5 (**4**)} or 1,1'-[Fe{(η^5-C_5H_4)CH=C(CN)COR}$_2$], {R = OEt (**2**), -NHN=C(CH_3)C_6H_5 (**5**)} in high yields. (Yields: **1**: 151 mg (98 %); **2**: 207 mg (96 %); **4**: 158 mg (80 %); **5**: 232 mg (76 %))

1: Anal. Calcd. ($C_{16}NO_2FeH_{15}$): C, 62.16; H, 4.89; N, 4.53, Found: C, 62.34; H, 4.82; N, 4.61. IR (ν_{CO}, cm^{-1},CH_2Cl_2): 2222 (s), 1749(s), 1721(vs), 1715 (vs), 1591 (s). ^{1}H NMR (δ, 400 MHz, $CDCl_3$): 1.40 (t, -CH_3, 3H, J=7.2 Hz), 4.28 (s, η^5-C_5H_5, 5H), 4.75 (t, η^5-C_5H_4, 2H, J=2 Hz), 5.05 (t, η^5-C_5H_4, 2H, J=2 Hz), 4.34 (q, CH_2, 2H, J=7.2 Hz), 8.21 (s, =CH, 1H). ^{13}C NMR (δ, 101 MHz, $CDCl_3$): 14.24 (-*C*H_3), 62.12 (-*C*H_2CH_3), 70.61 (η^5-*C*$_5H_5$), 71.82 (η^5-*C*$_5H_4$), 74.14 (η^5-*C*$_5H_4$), 97.13 (-*C*=C), 116.95 (-C=*C*-), 158.76 (-*C*N), 163.29 (-*C*=O). MS (ESI) m/z : Calculated ($C_{16}NO_2FeH_{15}$) 309.14; Found: 310.10 (M+H). UV-Vis λ_{max} (nm, ε (Mol^{-1} cm^{-1}): 267 (52000), 320 (43500), 380 (7200), 510 (7500).

2: Anal. Calcd. ($C_{22}N_2O_4FeH_{20}$): C, 61.13; H, 4.66; N, 6.48, Found: C, 61.38; H, 4.54; N, 6.59. IR (ν_{CO}, cm^{-1},CH_2Cl_2): 2223(m), 1723(vs), 1600 (vs). ^{1}H NMR (δ, 400 MHz, $CDCl_3$): 1.41 (t, CH_3, 3H, J= 7.2 Hz), 4.75 (t, η^5-C_5*H*$_4$, 4H, J = 2Hz), 4.36 (q, -C*H*$_2$, 4H, J= 7.2 Hz), 5.13 (t, η^5-C_5*H*$_4$, 4H, J = 2 Hz), 8.04 (s, =CH, 2H). ^{13}C NMR (δ, 101 MHz, $CDCl_3$): 14.16 (-*C*H_3), 62.46 (-*C*H_2CH_3), 73.35 (η^5-*C*$_5H_4$), 75.30 (η^5-*C*$_5H_4$), 76.02 (η^5-*C*$_5H_4$), 100.54 (-*C*=C),

116.15 (-C=*C*-), 155.72 (-*C*N), 162.43 (*C*=O). MS (ESI) m/z : Calculated ($C_{22}N_2O_4FeH_{20}$) 432.25; Found: 433.03 (M+H). UV-Vis λ_{max} (nm, ε (Mol^{-1} cm^{-1}): 280 (77000), 335 (60500), 425 (8700), 521 (9000).

4: Anal. Calcd. ($C_{22}N_3OFeH_{19}$): C, 66.52; H, 4.82; N, 10.58, Found: C, 66.75; H, 4.89; N, 10.70. IR(ν_{CO}, cm^{-1},CH_2Cl_2): 2211 (m), 1730(vs), 1712(s),1669(s), 1585(s). ^{1}H NMR (δ, 400 MHz, $CDCl_3$): 2.38 (s, CH_3, 3H), 4.30 (s, η^5-C_5H_4, 5H), 4.78(s, η^5-C_5H_4, 2H), 5.05(s, η^5-C_5H_4, 2H), 7.43 – 7.82 (m, C_6H_5, 5H), 8.46 (s, =CH, 1H), 9.15 (s, NH, 1H). MS (ESI) m/z: Calculated ($C_{22}N_3OFeH_{19}$) 397.25; Found: 399.26 (M+2H), 398.17 (M+H).

5: Anal. Calcd. ($C_{34}N_6O_2FeH_{28}$): C, 67.11; H, 4.64; N, 13.81, Found: C, 67.26; H, 4.55; N, 13.86. IR (ν_{CO}, cm^{-1},CH_2Cl_2): 2213 (m), 1693(s), 1673(s), 1667(vs), 1650(s). ^{1}H NMR (δ, 400 MHz, $CDCl_3$): 4.74 (s, η^5-C_5H_4, 4H), 5.15(s, η^5-C_5H_4, 4H), 7.30 – 7.68 (m, C_6H_5, 5H), 8.21(s, =C*H*, 2H), 9.26 (s, NH, 2H). MS (ESI) m/z : Calculated ($C_{34}N_6O_2FeH_{28}$) 608.47; Found: 609.16 (M+H).

*1.3. Synthesis of [{(C_6H_5)C(CH_3)=NNHC(O)CH_2CN}] (**3**)*

In a 100 ml round bottomed flask or conical flask containing 1 gm of Rice Husk ash (RHA), dichloromethane solution of cyanoacetyl hydrazide (0.12 mmol) was added and the mixture was thoroughly mixed using magnetic stirrer. Solvent was evaporated to dryness using vacuum to obtain a solid mixture. Acetophenone (0.1mmol) was then added and stirred continuously for five hours at 40° C. After the reaction, the solid mixture was cooled and extracted in dichloromethane solvent and dried in vacuum. The residue was then dissolved in dichloromethane and subjected to chromatographic work

up using a short column chromatography. Rapid elution with 20% ethylacetate : n-hexane solvent mixture afforded the compound [{$(C_6H_5)C(CH_3)$═$NNHC(O)CH_2CN$}] (**3**).

3: IR (ν_{CO}, cm^{-1}, CH_2Cl_2): 2222 (m), 1693 (vs), 1640 (s), 1632 (m). ^1H NMR (δ, 400 MHz, $CDCl_3$): 2.29 (s, CH_3, 3H), 3.93(s, CH_2, 2H), 7.42 – 7.73(m, 5H), 9.23 (s, NH, 1H).

Spectral data matched with those previously reported.[2]

*1.4. Crystal structure determination for **2***

Single crystal X-ray structural studies of **2** were performed on a CCD Oxford Diffraction XCALIBUR-S diffractometer equipped with an Oxford Instruments low-temperature attachment. Data were collected at 150(2) K using graphite-monochromated Mo Kα radiation (λ_α = 0.71073 Å). The strategy for the data collection was evaluated by using the CrysAlisPro CCD software. The data were collected by the standard 'phi-omega scan techniques, and were scaled and reduced using CrysAlisPro RED software. The structures were solved by direct methods using SHELXS-97 and refined by full matrix least-squares with SHELXL-97, refining on F^2.[3] The positions of all the atoms were obtained by direct methods. All non-hydrogen atoms were refined anisotropically. The remaining hydrogen atoms were placed in geometrically constrained positions and refined with isotropic temperature factors, generally 1.2U_{eq} of their parent atoms.

1.5. Solar cell fabrication

Fluorine-doped tin oxide (FTO) coated glass (Sigma Aldrich TEC A7) was cleaned by detergent, DI water, acetone, and ethanol using ultrasonic cleaner, and then dried. Cleaned FTO coated glass substrates underwent UV-ozone treatment for 30 min prior to the deposition of compact TiO_2 hole-blocking layer. A mildly acidic solution of Titanium isopropoxide in ethanol was spin coated on substrates for 45 seconds at 2000 rpm to deposit the compact TiO_2 layer. Then the coated film was dried at 150°C for 20 minutes followed by annealing at 450°C for 30 minutes. Commercially available TiO_2 paste (Dysesole 18NR-T) was diluted in ethanol and spin coated at 1500 rpm for 60 s to get the meso-TiO_2 electron transporting layer of thickness about 2 µm. The deposited film was dried at 200°C for 15 min and finally annealed at 550°C for 45 min. Meso-TiO_2 coated FTO photo-anode was also treated with UV-ozone treatment before compound loading. The TiO_2 layer was sensitized by immersing the meso-TiO_2 coated substrate into a 0.01M dichloromethane solution of **1** or **2** for 12 hours followed by drying the sample under vacuum for another 12 hours. Finally, circular Pt electrodes (80 nm thick) of diameter 1 mm were deposited by thermal evaporation through a shadow mask on the sample to complete the device fabrication.

1.6. J-V measurement:

The current density vs voltage (*J-V*) characteristics was measured using keithely 2400 source meter with the labtrcer 2.0 software under the illumination of 100 mW/cm^2 (AM 1.5G) from a solar simulator (Class AAA solar simulator, Model 94063A, Oriel) and a calibrated Si-reference cell certificated by NREL. Diode characteristics in dark condition as well as under illumination condition was measured using the same fabricated device.

1.7. Computational details

DFT calculations was carried out using Gaussian 09 (Version: ES64L-G09RevE.01) with LANL2DZ basis set at B3LYP level of theory. Geometry optimization of compounds **1** and **2** and their oxidized species (**1**$^{+}$**, 2**$^{+}$) was carried out in gas phase by density functional theory (DFT) at B3LYP level using LANL2DZ basis sets. The Natural electron population analysis (NPA) was also performed on **1** and **2** as well as on their respective 1e^{-}-oxidized species using the same basis set. The spectroscopic and electronic property of these complexes has been computed by time dependent DFT (TD-DFT) calculation at the same B3LYP level in gaseous phase.[4] Frequency calculation has been done at the same level of theory and found that the number of imaginary frequency is zero.

1.8. References:

1. Mueller-Westerhoff, U. T.; Yang, Z.; Ingram, G. A simple synthesis of metallocene aldehydes from lithiometallocenes and N,N-dimethylformamide: Ferrocene and ruthenocene aldehydes and 1,1′-dialdehydes. *J. Organomet. Chem.* **1993**, *463*, 163-167.

2. (a) Zelenin, K. N.; Oleinik, S. V.; Alekseev, V. V.; Potekhin, A. A. Structure of cyanoacetylhydrazones of aldehydes and ketones. *Russ. J. General Chem.* **2001**, *71*, 1116-1120.

3. Sheldrick, G. M. A short history of SHELX, *Acta Cryst. A* **2008**, *64*, 112-122.

4. (a) Becke, A. D.; *J. Chem. Phys.* **1993**, *98*, 5648. (b) Lee, A.; Yang, W.; Parr, R. G. *Phys. Rev. B* **1988**, *37*, 785. (c) Ghosh, A.; Halvorsen, I.; Nilsen, H. J.; Steene, E.; Wondimagegn, T.; Lie, R.; Caemelbecke, E.; Guo, N.; Ou, Z.; Kadish, K. M. *Phys. Chem. B* **2001**, *105*, 8120.